Journal of Heat and Mass Transfer Research 3 (2016) 115-129

Semnan University

Journal of Heat and Mass Transfer Research

Journal homepage: http://jhmtr.journals.semnan.ac.ir

A Comparative Solution of Natural Convection in an Open Cavity using Different Boundary Conditions via the Lattice Boltzmann Method

Mohsen Nazari* and Mohammad Hassan Kayhani

Department of Mechanical Engineering, Shahrood University of Technology, Shahrood, IRAN.
P.O. Box: 3619995161, nazari_me@yahoo.com

PAPER INFO

History:

Submitted 25 March 2014
Revised 1April 2016
Accepted 27 September 2016

Keywords:

Natural convection
Lattice Boltzmann method
Open cavity
Hydrodynamic boundary conditions
Thermal boundary conditions

A B S T R A C T

A lattice Boltzmann method is applied to compare the results of simulating natural convection in an open-end cavity using different hydrodynamic and thermal boundary conditions. The Prandtl number in the present simulation is 0.71, Rayleigh numbers are 104,105, and 106, and selected viscosities are 0.02 and 0.05. The on-grid bounce-back method with first-order accuracy and the no-slip method with second-order accuracy are employed for implementation of hydrodynamic boundary conditions. Moreover, two different thermal boundary conditions (with first- and second-order accuracy) also are presented for thermal modelling. The results showed that first- and second-order boundary conditions (thermal/hydrodynamic) are the same for a two-dimensional, single-phase, convective-heat transfer problem, including geometry with straight walls. The obtained results for different hydrodynamic and thermal boundary conditions are useful for researchers in the field of the lattice Boltzmann method in order to implement accurate conditions on the boundaries with different physics.

DOI: 10.22075/jhmtr.2016.363

1. Introduction

Natural convection in cavities has many engineering applications, such as solar collectors and heat exchangers. There have been some publications related to natural heat transfer in closed- and open-end cavities. Chan and Tien [1] performed a numerical study on natural convection in shallow open cavities. Bilgen and Muftuoglu [2] investigated natural heat transfer in a cavity with slots.

Recently, the lattice Boltzmann method has been used as an applicable alternative to classic methods, such as the finite-volume method. An advantage of the lattice Boltzmann method over others is its ease in calculation and boundary conditionings. Many works have studied natural convections in enclosures using the lattice Boltzmann method. There are many studies about applying boundary conditions in the lattice Boltzmann method [3-10]. Hydrodynamic boundary conditions have interested many researchers [11-12]. Ziegler [13] developed a new approach for no-slip boundary conditions for the lattice Boltzmann and lattice gas simulations. Nobel et al. [14] presented a hydrodynamic boundary condition as an alternative to the bounce-back boundary condition, which is used in most lattice Boltzmann simulations. In that study, an incompressible fluid flows between two parallel plates, and the boundary condition is applied to the two-dimensional steady flow. Chen et al. [15] used an extrapolation to develop a boundary condition to simulate the fluid flow. They considered the lattice

Corresponding Author: Mohsen Nazari *Department of Mechanical Engineering, Shahrood University of Technology, Shahrood, IRAN*
Email: nazari_me@yahoo.com

Boltzmann method to be a specific finite difference scheme for the kinetic equation of the discrete velocity distribution function.

A thermal boundary condition also has been studied in many researches [16-20]. D'Orazio et al. [10] proposed a novel thermal boundary condition, which can be applied in the case of either a constant wall temperature (Dirichlet boundary condition) or a constant heat flux on the wall (Newman boundary condition). D'Orazio and Succi [21] proposed a thermal boundary condition in which the unknown distribution functions are considered to be the equilibrium distribution functions with a counter-slip internal energy and developed thermal boundary conditions for both Dirichlet and Newmann conditions. A second-order accuracy thermal boundary condition was developed by Kuo and Chen [22] using a nonequilibrium mirror-reflection scheme. They also investigated properties of the temperature gradient that were calculated directly from the thermal lattice Boltzmann method.

Natural convection heat transfer in an open-end cavity has been studied by applying the lattice Boltzman Method [23]. In that study, the D2Q9 model was used for flow while a D2Q4 model was applied for temperature. The bounce-back boundary condition (first-order accuracy) was used for flow on the solid walls, and since the north and south walls were insulated, the bounce-back boundary condition (adiabatic) for temperature was applied on these walls. The boundary condition of the west wall was calculated using the wall temperature. Dixit and Babu [24] used the lattice Boltzmann method to simulate natural-convection heat transfer with a high Rayleigh number in a square cavity. In that study, a standard D2Q9 model was used for both flow and temperature. As for the boundary conditioning, for both flow and temperature, a no-slip boundary condition (second-order accuracy) was applied on all walls. The north and south walls were adiabatic, while west and east walls were maintained at constant but different temperatures. Double diffusive natural convection has been studied in an open-end cavity using the lattice Boltzmann method [25]. In this study, south and north walls were insulated, and the left wall was at a constant temperature (the right side was open). A D2Q9 model was applied for the flow while a D2Q4 model was used for temperature and species concentration. In this work, for the flow, the bounce-back boundary condition was imposed on solid walls, and since north and south walls were adiabatic (or have no flux), this type of boundary condition also was used on these walls for temperature (or concentration). The boundary condition of the west wall was calculated using a constant wall temperature (or concentration).

The current study presents comparative results of simulated natural convection with different boundary conditions for flow in an open-end cavity using the lattice Boltzmann Method. The results show accuracy of each boundary condition and their accordance to one another. Comparisons between different thermal and hydrodynamic boundary conditions, with different orders of accuracy, have not been presented completely in the literature, and this topic, to the best of our knowledge, is an open research topic.

2. Method of solution

In this work, a simple D2Q9 algorithm is used for both flow and temperature. Fig. 1 shows the cavity boundaries and the known and unknown distribution functions. South and north walls are adiabatic (zero-temperature gradient), while east and west walls have constant temperatures.

Flow streaming and collision are presented as the following [26, 27]:

$$f_a\left(x+\vec{e_a}\Delta t, t+\Delta t\right)=f_a\left(x,t\right)-\frac{\left[f_a\left(x,t\right)-f_a^{eq}\left(x\,t\right)\right]}{\tau}+\Delta t.\vec{F_a}, \quad (1)$$

where $f_a\left(x+\vec{e_a}\Delta t, t+\Delta t\right)$ is the streaming part and the right-hand side of the equation is the collision term. f_a^{eq} is the equilibrium distribution function, and τ is the relaxation time. The equilibrium distribution function f_a^{eq} is given by

$$f_a^{eq}\left(x\right)=\omega_a\rho\left(x\right)\left[1+3\frac{\vec{e_a}\vec{u}}{c^2}+\frac{9}{2}\frac{\left(\vec{e_a}\vec{u}\right)^2}{c^4}-\frac{3}{2}\frac{\vec{u}.\vec{u}}{c^2}\right], \quad (2)$$

where ρ and $\vec{u}$ are density and microscopic velocity, respectively, and ω_a are the weight factors, which, for the D_2Q_9 model, are defined as

$$\omega_a=\begin{cases}4/9 & a=0\\ 1/9 & a=1,2,3,4\\ 1/36 & a=5,6,7,8\end{cases}. \quad (3)$$

The velocities $\vec{e_a}$ are [23]

$$\vec{e}_a = \begin{cases} 0 & a = 0 \\ c(\cos\theta_a, \sin\theta_a) & \theta_a = (a-1)\frac{\pi}{2} \quad a = 1,2,3,4 \\ c\sqrt{2}(\cos\theta_a, \sin\theta_a) & \theta_a = (a-5)\frac{\pi}{2} + \frac{\pi}{4} \quad a = 5,6,7,8 \end{cases} \quad (4)$$

,

where c = Δx/Δt, Δx is the lattice space, and Δt is the lattice time step size. In Eq. (1), $\overrightarrow{F_a}$ is the force term in each of the directions and can be defined as

$$\overrightarrow{F_a} = \omega_a \vec{F} . \frac{\overrightarrow{e_a}}{c_s^2} , \quad (5)$$

where $\vec{F}$ is defined as

$$\vec{F} = \rho \overrightarrow{g_r} \beta \Delta T , \quad (6)$$

where β, $\overrightarrow{g_r}$, and ΔT are the thermal expansion coefficient, gravity acceleration, and temperature difference, respectively. The macroscopic velocity $\vec{u}$ and density ρ can be obtained through the first and zeroth moment of the particle distribution f, i.e. [26, 27],

$$\vec{u} = \frac{1}{\rho} \sum_{a=0}^{8} f_a \overrightarrow{e_a} \quad (7)$$

$$\rho = \sum_{a=0}^{8} f_a . \quad (8)$$

The kinematic viscosity in the D2Q9 method is defined as [26, 27]

$$\upsilon = \left[\tau - \frac{1}{2} \right] c_s^2 \Delta t , \quad (9)$$

where c_s is the sound velocity, which is $c_s = \frac{c}{\sqrt{3}}$.

Temperature streaming and collision are presented as the following [23]:

$$g_a(x + \Delta x, t + \Delta t) = g_a(x,t)(1-\omega_s) + \omega_s g_a^{eq}(x,t) \quad (10)$$

where $g_a^{eq}(x,t)$ is the thermal equilibrium distribution function and ω_s is the relaxation time. The thermal equilibrium distribution function is defined as

$$g_a^{eq} = \omega_a T(x,t)[1 + \frac{\overrightarrow{e_a}\vec{u}}{c_s^2}] . \quad (11)$$

ω_s for the D2Q9 model is given by

$$\omega_s = \frac{1}{3\alpha + 0.5} , \quad (12)$$

where α is the thermal diffusion coefficient. The temperature, then, can be calculated at any point of the domain:

$$T = \sum_{a=0}^{8} g_a . \quad (13)$$

The average Nusselt number also is defined as

$$Nu = \frac{1}{M} \sum_{k=1}^{M} -\frac{\partial T}{\partial X} , \quad (14)$$

where *M* is the number of lattice nodes on the *Y* direction.

3. Boundary conditions

In this study, two different hydrodynamic boundary conditions in the presence of two types of thermal boundary conditions have been used. Here, the bounce-back boundary condition is compared with a no-slip boundary condition, and two different thermal boundary conditions—one with first-order accuracy and the other with second-order accuracy—are compared with each other. The term "bounce-back" is used here to mean bounce-back at the nodes (or "on-node bounce back"), which coincides with the actual physical boundaries. It should be noted that the mentioned "bounce-back" rule is different from the "link bounce-back." In the link bounce-back method, the boundary nodes lie midway between the solid and fluid nodes, and the fluid particles moving along the links between solid and fluid nodes interact at these boundary nodes.

3.1 Hydrodynamic boundary conditions

At the east wall, a zero gradient is realized through the following conditions:

$$\begin{aligned} f_{3,n} &= f_{3,n-1} \\ f_{6,n} &= f_{6,n-1} \\ f_{7,n} &= f_{7,n-1} , \end{aligned} \quad (15)$$

where *n* is the number of lattice nodes on the open wall and *n-1* is number of the lattice nodes next to the boundary inside the cavity. For solid walls, two different boundary conditions are used.

3.1.1 Bounce-back boundary condition

On the solid walls (west, south, and north boundaries), the bounce-back boundary condition is used. For instance, at the south wall, the unknown distribution functions would be f_2, f_5 *and* f_6, which are

$$\begin{aligned} f_{2,n} &= f_{4,n} \\ f_{5,n} &= f_{7,n} \\ f_{6,n} &= f_{8,n} \end{aligned} \quad (16)$$

where *n* is the number of lattice nodes on the south wall.

3.1.2 A no-slip boundary condition

The lattice Boltzmann method is a method with second-order accuracy. The bounce-back boundary condition for applying zero velocity at a wall is a method of first-order accuracy. This shows that using the bounce-back boundary condition is not always the best choice for boundary conditioning in the lattice Boltzmann method. Second-order accuracy in the bounce-back method is achieved if there are straight walls, and we correct for the shift in the effective position of the wall. If τ = 1 and there is a straight wall, the effective wall is always at half the distance between fluid and solid boundary nodes, so that is fine. For simple flows (like a Poiseuille flow), the shift of the wall even can be computed analytically for a given τ . However, in our case, that is not so straightforward; therefore, we return to a first-order accuracy. Here, a no-slip boundary condition is used to overcome this issue, which is a second-order accuracy method. In this method, unknown distribution functions are assumed to be an equilibrium distribution function with a counter-slip velocity, which is determined so that fluid velocity at the wall is equal to the wall velocity. The velocity normal to the wall is equal to the velocity of the wall, while the velocity along the wall is not equal to that of the wall. The difference between the wall velocity and the velocity along the wall is called slip velocity.

For the south wall, the unknown distribution functions are f_2, f_5 *and* f_6, which are defined as [3]

$$\begin{aligned} f_2 &= \tfrac{1}{9}\rho'\left[1+3v_w+\frac{9}{2}v_w^2-\frac{3}{2}\left[(u_w+u')^2+v_w^2\right]\right] \\ f_5 &= \tfrac{1}{36}\rho'\left[1+3(u_w+u'+v_w)+\frac{9}{2}(u_w+u'+v_w)^2-\frac{3}{2}\left[(u_w+u')^2+v_w^2\right]\right] \\ f_6 &= \tfrac{1}{36}\rho'\left[1+3(-u_w-u'+v_w)+\frac{9}{2}(-u_w-u'+v_w)^2-\frac{3}{2}\left[(u_w+u')^2+v_w^2\right]\right] \end{aligned} \quad (17)$$

,

where u_w and v_w are the velocity of the wall in x and y directions, respectively, and ρ' and u' are unknown parameters, which can be defined by the condition that fluid velocity on the wall is equal to that of the wall. u' is the counter-slip velocity. Now, we have two equations for u_w and v_w and one equation for ρ_w (density of the virtual fluid in the wall), which can be calculated using Eq. (8). Thus, the unknown parameters are:

$$\begin{aligned} \rho_w &= \frac{1}{1-v_w}\left[f_0+f_1+f_3+2(f_4+f_7+f_8)\right] \\ \rho' &= 6\frac{\rho_w v_w+(f_4+f_7+f_8)}{1+3v_w+3v_w^2} \\ u' &= \frac{1}{1+3v_w}\left[6\frac{\rho_w u_w-(f_1-f_3+f_8-f_7)}{\rho'}-u_w-3u_w v_w\right] \end{aligned} \quad (18)$$

.

Since $u_w = v_w = 0$, the unknown distributions are

$$\begin{aligned} f_2 &= \rho'\left(\frac{1}{9}-\frac{1}{6}u'^2\right) \\ f_5 &= \rho'\left(\frac{1}{36}+\frac{1}{12}u'+\frac{1}{12}u'^2\right) \\ f_6 &= \rho'\left(\frac{1}{36}-\frac{1}{12}u'+\frac{1}{12}u'^2\right). \end{aligned} \quad (19)$$

3.2 Thermal boundary conditions

At the east wall (open wall), the boundary condition depends on whether the flow penetrates the cavity or leaves it. If the flow penetrates the cavity, then the temperature should be ambient $T = 0$, and if the flow is leaving the cavity, there is no diffusion [23]. At the open wall, unknown distribution functions are

$$\begin{aligned} &\text{if } u \prec 0 \text{ then} \quad g_{3,n} = -g_{1.n} \quad g_{6,n} = -g_{8.n} \quad g_{7,n} = -g_{5.n} \\ &\text{if } u \succ 0 \text{ then} \quad g_{3,n} = g_{3.n-1} \quad g_{6,n} = g_{6.n-1} \quad g_{7,n} = g_{7.n-1} \end{aligned} \quad (20)$$

For solid walls two different boundary conditions with first- and second-order accuracy have been used.

3.2.1 First-order accuracy thermal boundary condition

For north and south walls (adiabatic walls), bounce-back boundary conditions are used. At the west wall ($T_w = 1$), the boundary condition can be calculated using the wall temperature:

$$\begin{aligned} g_{1,n} &= T_w\left(\omega_1 + \omega_3\right) - g_{3.n} \\ g_{5,n} &= T_w\left(\omega_5 + \omega_7\right) - g_{7.n} \\ g_{8,n} &= T_w\left(\omega_8 + \omega_6\right) - g_{6.n} \end{aligned} . \quad (21)$$

3.2.2 Second-order accuracy thermal boundary condition

Here, a thermal boundary condition (D'Orazio's approach [10]) is used, which is a second-order accuracy boundary condition. In this method, unknown distribution functions are assumed to be an equilibrium distribution function at a temperature T_0. The temperature T_0 is calculated considering whether the wall is insulated (Newman boundary condition) or has a constant temperature (Dirichlet boundary condition). Since we have a zero velocity on the walls, from Eq. (11) for unknown distributions, we have

$$g_a^{eq} = \omega_a T_0 . \quad (22)$$

For the west wall (the Dirichlet boundary condition), the unknown distribution functions are g_1, g_5, and g_8. According to Eq. (22), we have

$$\begin{aligned} g_1^{eq} &= \frac{1}{9}T_0 \\ g_5^{eq} &= \frac{1}{36}T_0 \\ g_8^{eq} &= \frac{1}{36}T_0 \end{aligned} \quad (23)$$

The wall temperature T_w is calculated using Eq. (13):

$$T_w = \sum_{a=0}^{8} g_a = T_p + \frac{1}{6}T_0 \quad (24)$$

where T_p is the sum of the known distribution functions:

$$T_p = g_0 + g_2 + g_3 + g_4 + g_6 + g_7 . \quad (25)$$

From Eq. (24), T_0 can be calculated as

$$T_0 = 6\left(T_w - T_p\right) \quad (26)$$

and unknown distribution functions are

$$\begin{aligned} g_1 &= \frac{2}{3}\left(T_w - T_p\right) \\ g_5 &= \frac{1}{6}\left(T_w - T_p\right) \\ g_8 &= \frac{1}{6}\left(T_w - T_p\right) \end{aligned} \quad (27)$$

For insulated walls, there is no temperature gradient. For instance, on the north wall, the unknown distribution functions are g_4, g_7, and g_8. Using Eq. (22), we have

$$\begin{aligned} g_4^{eq} &= \frac{1}{9}T_0 \\ g_7^{eq} &= \frac{1}{36}T_0 \\ g_8^{eq} &= \frac{1}{36}T_0 \end{aligned} \quad (28)$$

$$T_0 = 6T_p \quad (29)$$

where T_p is defined by

$$T_p = g_2 + g_5 + g_6 . \quad (30)$$

Therefore, the unknown distribution functions can be calculated by

$$\begin{aligned} g_4 &= \frac{2}{3}T_p \\ g_7 &= \frac{1}{6}T_p \\ g_8 &= \frac{1}{6}T_p \end{aligned} \quad (31)$$

4. Results and discussion

This study compared two hydrodynamic and two thermal boundary conditions in order to find the most convenient one. For this purpose, some features, such as the Nusselt number, velocity, and

temperature at the center of the cavity, were compared with each other in different cases using all methods. From these figures, we can understand the differences and similarities of these methods' influences on the mentioned features, and as can be seen, one can simply use the bounce-back boundary condition for flow and the first-order accuracy thermal boundary condition instead of the more complicated no-slip boundary condition and second-order accuracy thermal boundary condition.

Table 1. Nusselt number comparison resulting from different hydrodynamic methods in the presence of the first-order accuracy thermal boundary condition in the case of viscosity = 0.02

Ra		LBM/Error(%) grid=64×64	LBM /Error(%) grid=128×128	LBM/Error(%) grid=256×256	Mohamad [23] LBM	Mohamad [30] FVM	Hinojosa et. al [31] FVM
10^4	Bounce Back	3.297/1.016	3.283/0.596	3.361/2.977	3.377	3.264	3.57
	No Slip	3.299/1.082	3.284/0.612	3.361/2.981			
10^5	Bounce Back	7.254/0.095	7.250/0.017	7.256/0.064	7.323	7.261	7.75
	No Slip	7.257/0.054	7.261/0.003	7.257/0.059			
10^6	Bounce Back	14.19/0.843	14.33/1.831	14.33/1.839	14.38	14.076	15.11
	No Slip	-	14.33/1.839	14.33/1.843			

The errors are calculated with respect to the F.V. solution [30]. The numbers of lattices in [23] are 64*64, 128*128 and 256*256 for the Ra. Numbers of 10^4, 10^5, and 10^6, respectively.

Table 2. Nusselt number comparison resulting from different types of boundary conditions in the case of viscosity = 0.05 and Ra = 10^5

Type of boundary condition	Nu		
	grid=64×64	grid=128×128	grid=256×256
flow=B.B & Temperature=1st order accuracy	7.244257	7.257607	7.246472
flow=No-slip & Temperature=1st order accuracy	7.242551	7.257314	7.246411
flow=B.B & Temperature=2nd order accuracy	7.253804	7.263481	7.255821
flow=No-slip & Temperature=2nd order accuracy	7.252012	7.263239	7.255728

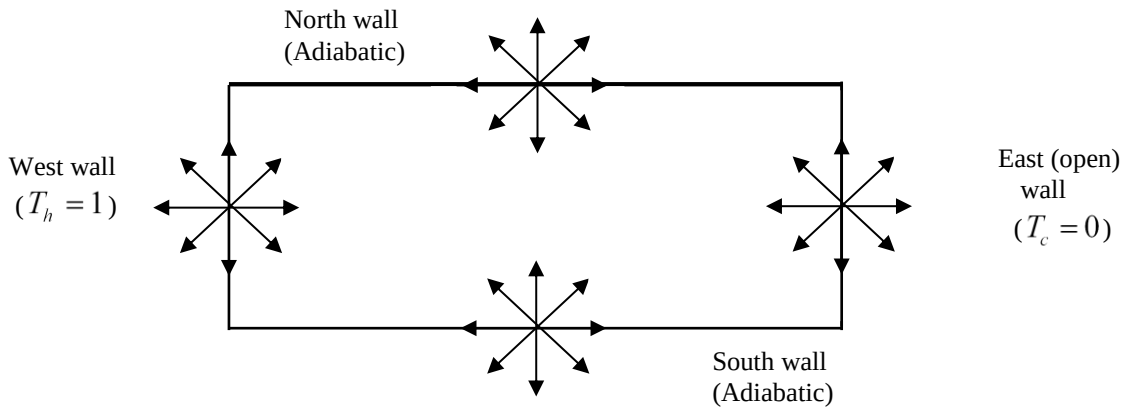

Fig.1 Cavity boundaries and velocity

Table 1 illustrates the comparison of the Nusselt number in both types of hydrodynamic boundary conditions in the presence of the first-order accuracy thermal boundary condition in the case of different Rayleigh numbers and the number of lattice nodes. This table also includes the Nusselt numbers reported by other authors using the lattice Boltzmann method and finite-volume method. One can see that the Nusselt number resulting from this study is in good agreement with the Nusselt number resulting from the mentioned works. Table 2 shows the Nusselt number using all of the mentioned thermal and hydrodynamic boundary conditions. As can be seen in this table, in a certain viscosity, the Nusselt numbers calculated using different combinations of thermal and hydrodynamic boundary conditions are almost equal in all cases of grid numbers (number of lattice nodes).

Figs. 2 and 3 illustrate the streamlines and isotherms, respectively, for the cases of bounce-back and first-order accuracy thermal boundary conditions for $Ra = 10^5$ and $\upsilon = 0.05$. These visualizations of flow and temperature fields will help to understand the physics and the importance of the choice of boundary conditions.

The results for each type of boundary condition are presented in Figs. 4–14. In the figures, "visco," "B.B.," and "Temp" stand for "viscosity," "Bounce-back boundary condition," and "temperature," respectively. In Figs. 4–12, the applied thermal boundary condition is a first-order accuracy one. Figs. 4–6 show that Nusselt numbers at a fixed viscosity are almost the same for both bounce-back and no-slip boundary conditions.

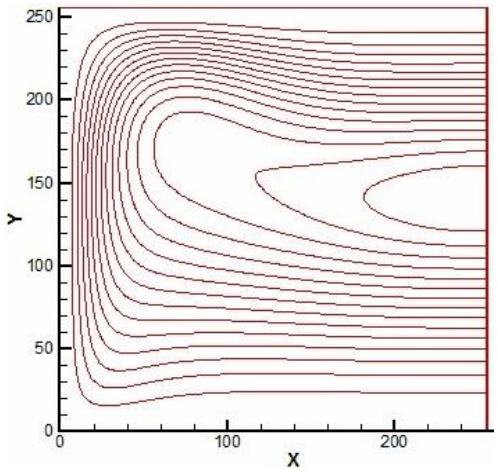

Fig.2 Streamlines in the case of bounce-back boundary conditions for Ra = 10^5 and υ = 0.05.

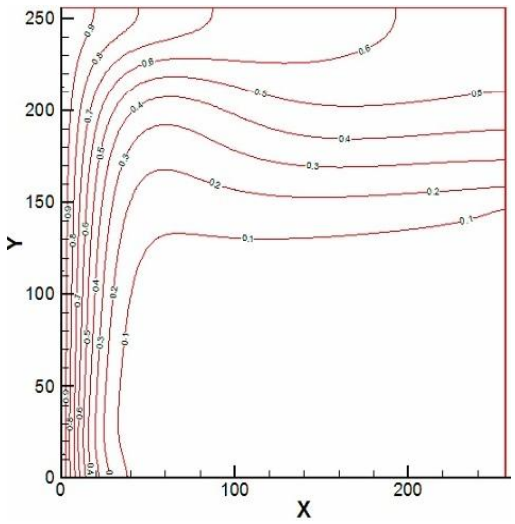

Fig.3 Isotherms in the case of bounce-back boundary conditions for Ra = 10^5 and υ = 0.05.

Moreover, the value of viscosity has little influence on the Nusselt number in both types of boundary conditions. In other words, the Nusselt number does not change with viscosity in either of the methods, and when it does, this mostly is seen along with high Rayleigh numbers. As it has been illustrated, the number of lattice nodes has little effect on the Nusselt number, and the Nusselt number is pretty much the same in all cases (a–c). Here the Nusselt number of the last iteration is used, and it does not change with iteration after this equilibrium time (number of iterations).

Figs. 7–9 illustrate the temperature at the center of the cavity. It can be observed that both bounce-back and no-slip boundary conditions have almost a similar effect on the temperature in a certain viscosity. Regarding (a), (b) and (c) in all figures, it can be seen that each case has a different behavior in the path to converging. One can see that, in the case of higher numbers of lattices, there is a greater difference between the temperature results in the two different viscosities. This difference decreases as the time steps (number of iterations) increase. The same result is observed when the Rayleigh number increases. It can be observed that, in the case of higher Rayleigh numbers in a certain number of lattices, there is more variance between the results of two different viscosities. But this variance is negligible.

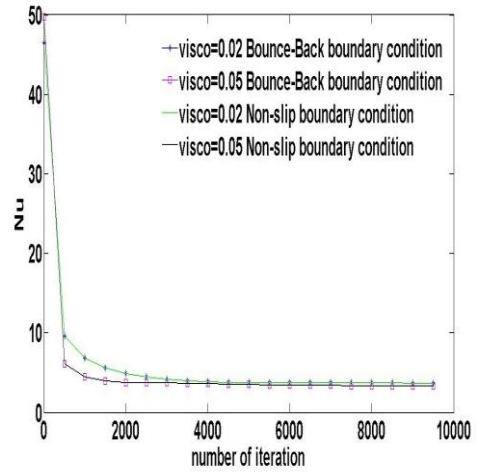

(a)

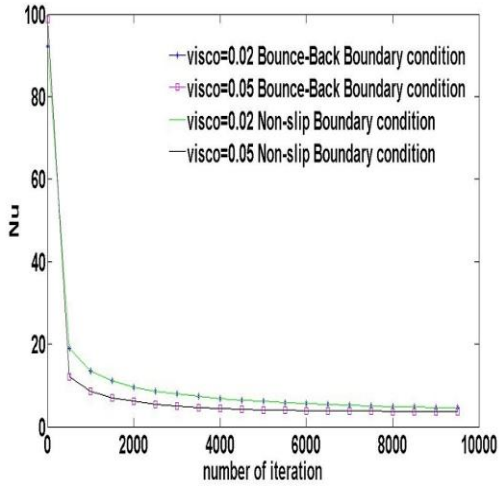

(b)

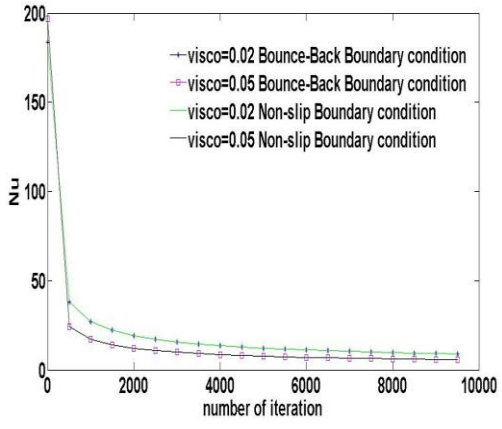

(c)

Fig.4 Nusselt number per iteration in the presence of the first-order accuracy thermal boundary condition at $Ra = 10^4$ for the number of lattice nodes on horizontal and vertical walls: a = 64×64, b = 128×128, and c = 256×256.

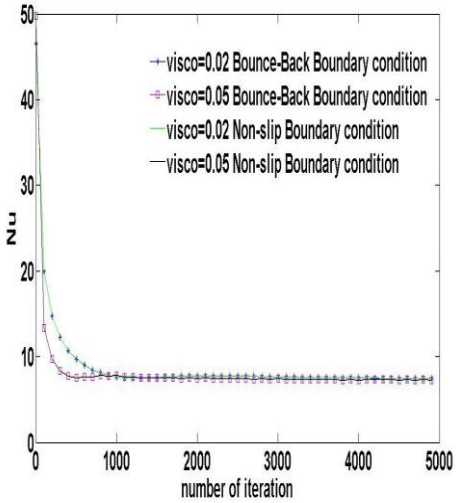

(a)

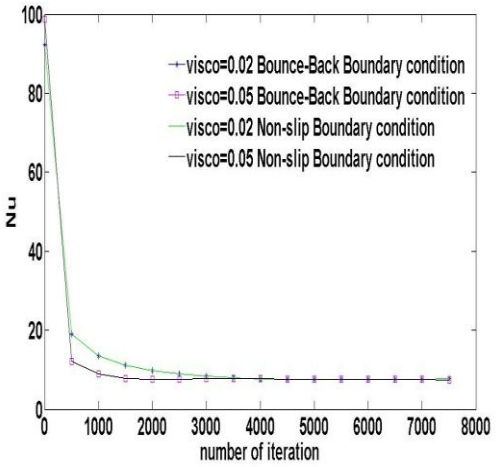

(b)

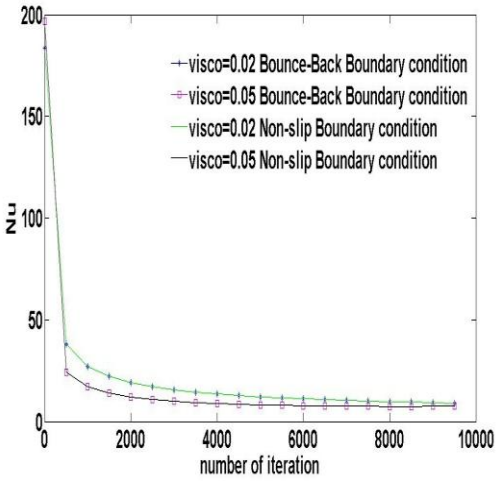

(c)

Fig.5 Nusselt number per iteration in the presence of the first-order accuracy thermal boundary condition at $Ra = 10^5$ for the number of lattice nodes on horizontal and vertical walls: a = 64×64, b = 128×128, and c = 256×256.

It also can be seen that in higher Rayleigh numbers, the path to a steady solution is oscillatory. It should be noted that, in the case of higher Rayleigh numbers, less time steps are required to reach convergence. When viscosity increases, the temperature at the center of the cavity increases, and this is true for both mentioned hydrodynamic boundary conditions. However, by decreasing viscosity, the time steps necessary to reach the convergence solution increases. This result is expected since the time scale is a function of υ (relaxation time) [29].

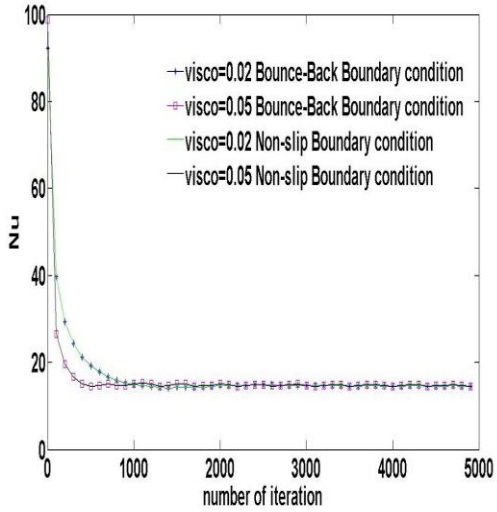

(a)

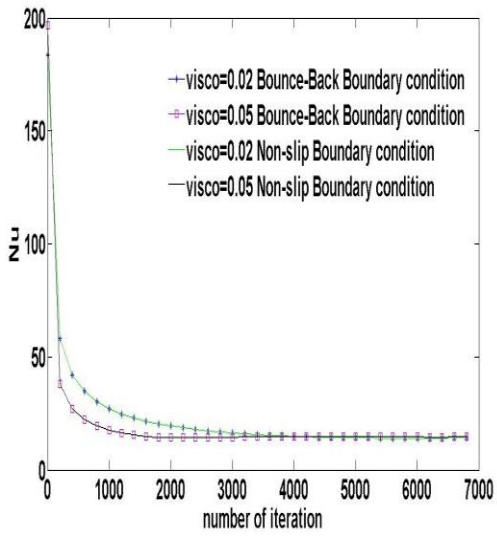

(b)

Fig.6 Nusselt number per iteration in the presence of the first-order accuracy thermal boundary condition at $Ra = 10^6$ for the number of lattice nodes on horizontal and vertical walls: a = 128×128 and b = 256×256.

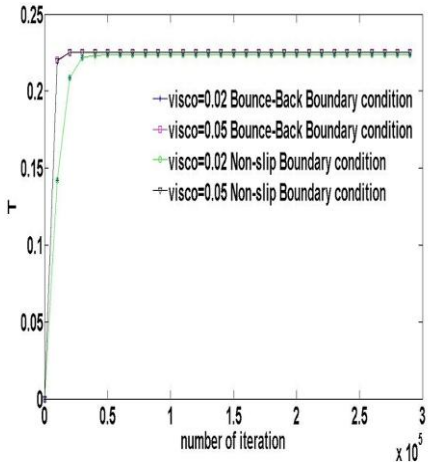

(a)

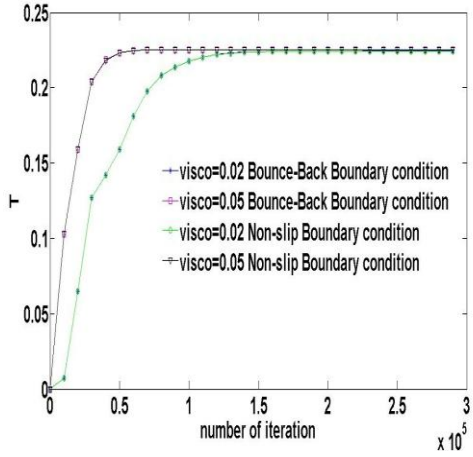

(b)

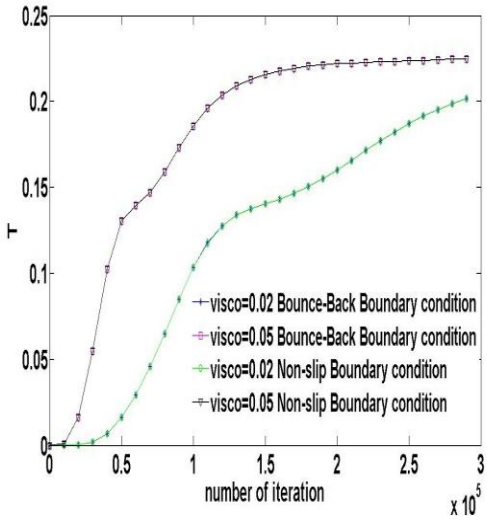

(c)

Fig.7 Temperature at the center of the cavity per iteration in the presence of the first-order accuracy thermal boundary condition at $Ra = 10^4$ for the number of lattice nodes on horizontal and vertical walls: a = 64×64, b = 128×128, and c = 256×256.

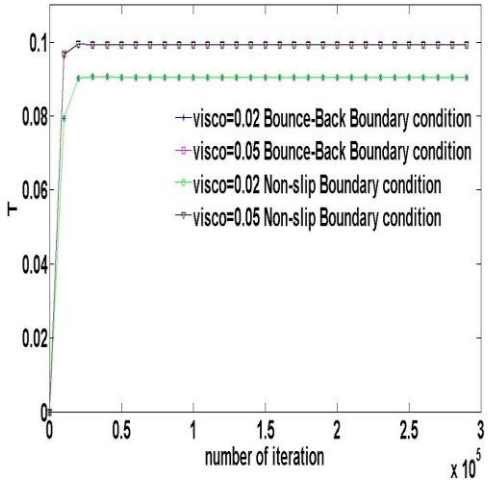

(a)

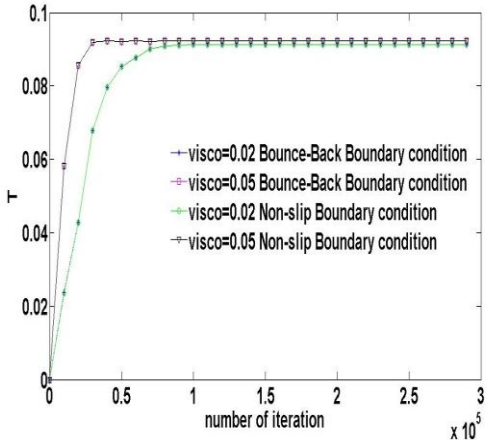

(b)

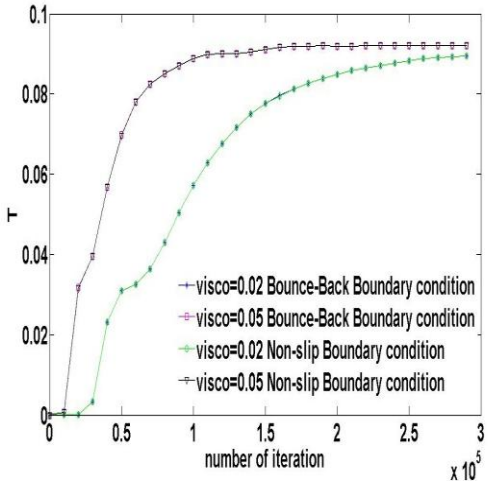

(c)

Fig.8 Temperature at the center of the cavity per iteration in the presence of the first-order accuracy thermal boundary condition at Ra = 10^5 for the number of lattice nodes on horizontal and vertical walls: a = 64×64, b = 128*128, and c = 256×256.

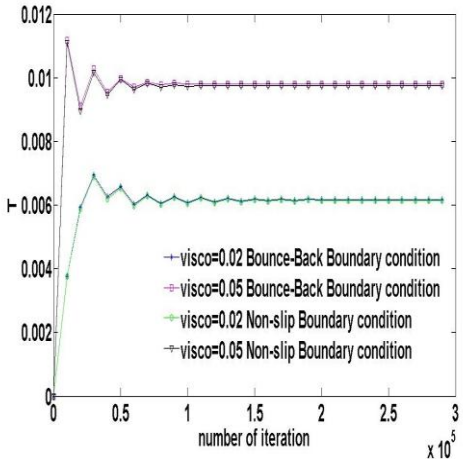

(a)

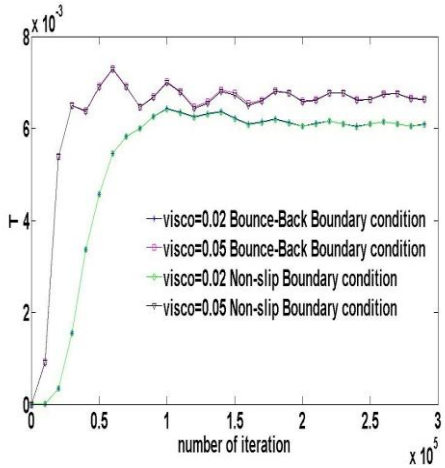

(b)

Fig.9 Temperature at the center of the cavity per iteration in the presence of the first-order accuracy thermal boundary condition at Ra = 10^6 for the number of lattice nodes on horizontal and vertical walls: a = 128×128 and b = 256×256.

Figs. 10–12 show changes in the velocity at the center of the cavity over the number of iterations for different Rayleigh numbers. On the one hand, it can be observed that, at higher Rayleigh numbers, it takes less time (less iterations) to reach a steady-state solution. On the other hand, by decreasing viscosity, the number of iterations for reaching the steady-state solution increases. The figures show that, in a certain viscosity, both mentioned boundary conditions have similar results. One can see that, in both types of hydrodynamic boundary conditions, the velocity at the center of the cavity is a negative value, and the absolute value of velocity in the case of viscosity = 0.02 is lower than of that in the case of viscosity = 0.05 (the ratio of velocity in the case of viscosity = 0.02 to that of viscosity = 0.05 is equal to 0.4).

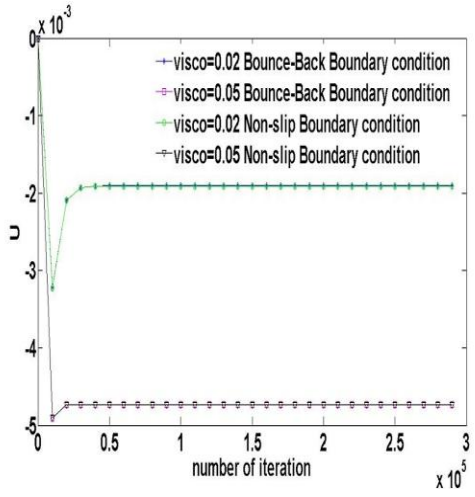

(a)

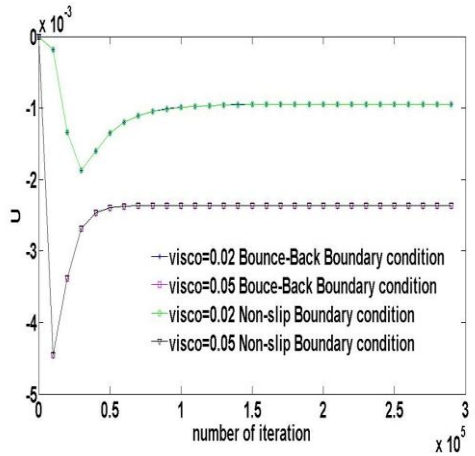

(b)

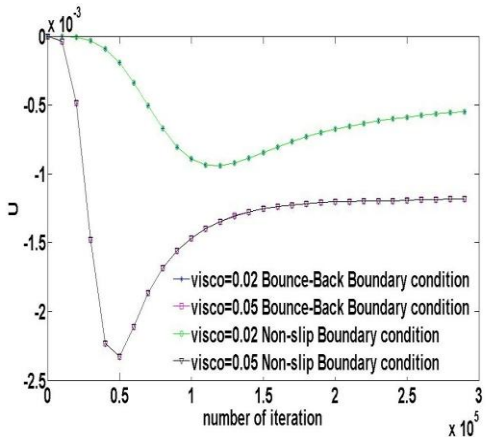

(c)

Fig.10 Velocity at the center of the cavity per iteration in the presence of the first-order accuracy thermal boundary condition at Ra = 10^4 for the number of lattice nodes on horizontal and vertical walls: a = 64×64, b = 128×128, and c = 256×256.

This is expected because, in the scaling process, the viscosity's conversion factor is a product of the conversion factors of velocity and length, and since M (the dimensionless value of length) is fixed in both cases, the conversion factor of length is constant, so the velocity ratio is equal to the viscosity ratio. Consider H as the height of the cavity, υ_{act} is the actual viscosity, and U_{act} is the actual velocity. Then, the conversion factors of length, viscosity, and velocity are defined as

$$\begin{aligned} C_H &= \frac{H}{M} \\ C_\upsilon &= \frac{\upsilon_{act}}{\upsilon} \\ C_u &= \frac{U_{act}}{U} \end{aligned} \tag{32}$$

where M is the number of lattice nodes (dimensionless value of length), υ is either 0.02 or 0.05, and U is the dimensionless velocity. Since dimensionless numbers (in this case, the Reynolds number) should be equal in both physical and dimensionless systems, the following applies:

$$\frac{U_{act} H}{\upsilon_{act}} = \frac{U.M}{\upsilon} . \tag{33}$$

Then from equations (32) and (33):

$$C_u = \frac{C_\upsilon}{C_H} , \tag{34-a}$$

or

$$\begin{cases} C_u = \left(\frac{1}{0.02}\right)\left(\frac{\upsilon_{act} M}{H}\right) & if \quad \upsilon = 0.02 \\ C_u = \left(\frac{1}{0.05}\right)\left(\frac{\upsilon_{act} M}{H}\right) & if \quad \upsilon = 0.05 \end{cases} \tag{34-b}$$

From equation (32):

$$\begin{cases} U1 = \frac{0.02 U_{act}.H}{\upsilon_{act} M} & if \quad \upsilon = 0.02 \\ U2 = \frac{0.05 U_{act}.H}{\upsilon_{act} M} & if \quad \upsilon = 0.05 \end{cases} \rightarrow \frac{U1}{U2} = \frac{0.02}{0.05} = 0.4 . \tag{35}$$

where $U1$ and $U2$ are the velocities in the case of viscosity = 0.02 and viscosity = 0.05, respectively.

Fig. 13 shows the effect of each type of boundary condition on variations of the Nusselt number with the number of iterations. One can see that Nusselt numbers at a fixed viscosity are almost the same for all boundary conditions. Therewith, the value of viscosity does not have much effect on the Nusselt number. In other words, the Nusselt number does not change with viscosity in any of the methods. As it has been illustrated, the number of lattice nodes has little effect on the Nusselt number, and the Nusselt number is pretty much the same in all cases (a–c).

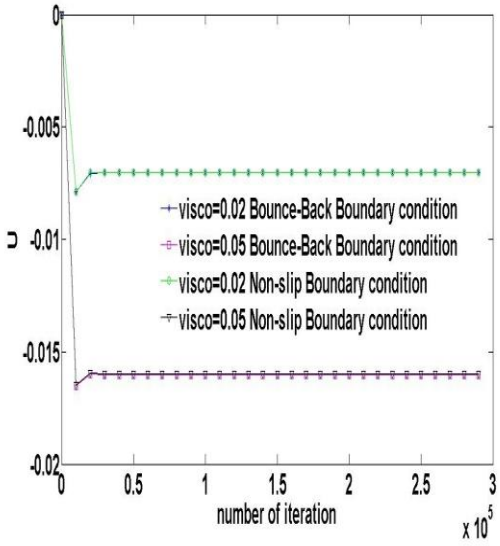

(a)

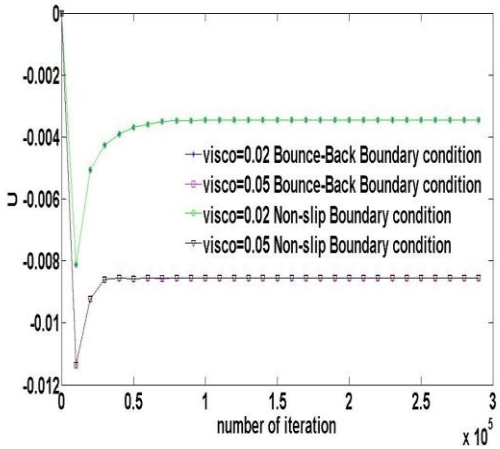

(b)

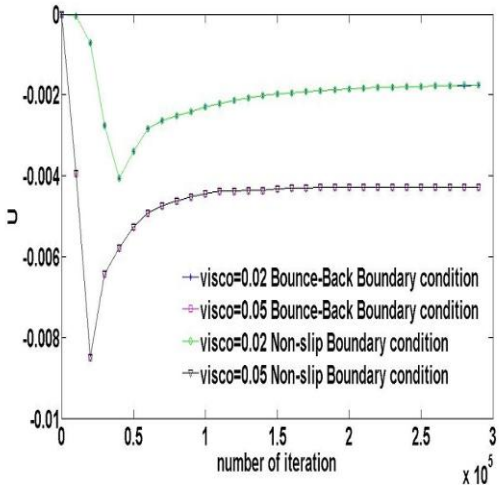

(c)

Fig.11 Velocity at the center of the cavity per iteration in the presence of the first-order accuracy thermal boundary condition at $Ra = 10^5$ for the number of lattice nodes on horizontal and vertical walls: a = 64×64, b = 128×128, and c = 256×256.

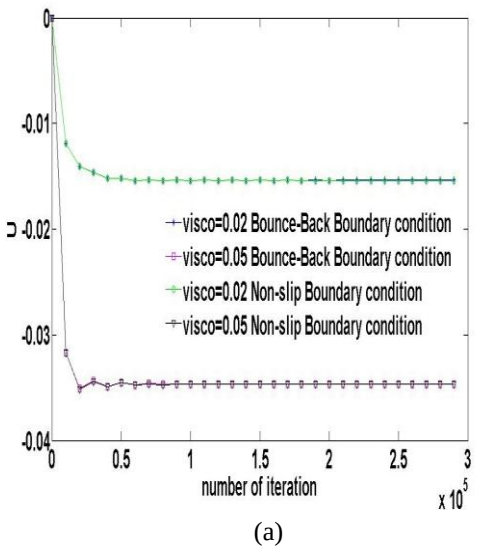

(a)

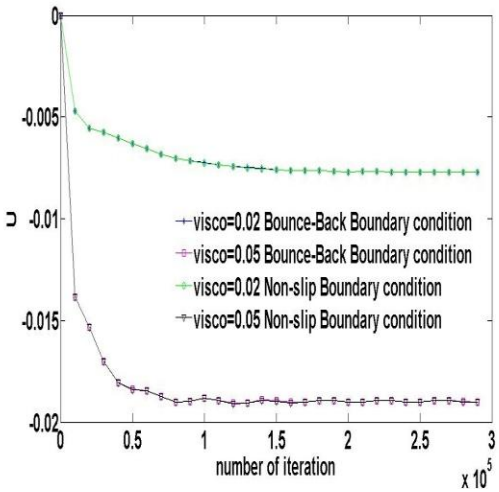

(b)

Fig.12 Velocity at the center of the cavity per iteration in the presence of the first-order accuracy thermal boundary condition at $Ra = 10^6$ for number of lattice nodes on horizontal and vertical walls: a = 128×128 and b = 256×256.

Fig. 14 illustrates the variation of the temperature at the center of the cavity with the number of iterations, using all mentioned thermal and hydrodynamic boundary conditions. It can be seen that all of the thermal and hydrodynamic boundary conditions have a nearly similar influence on the temperature in a certain value of viscosity. Moreover, the path to convergence changes with the number of lattice nodes. When there are more lattice nodes, there is a greater difference between the temperature results in the two different viscosities, with this difference decreasing as time steps (number of iterations) increase.

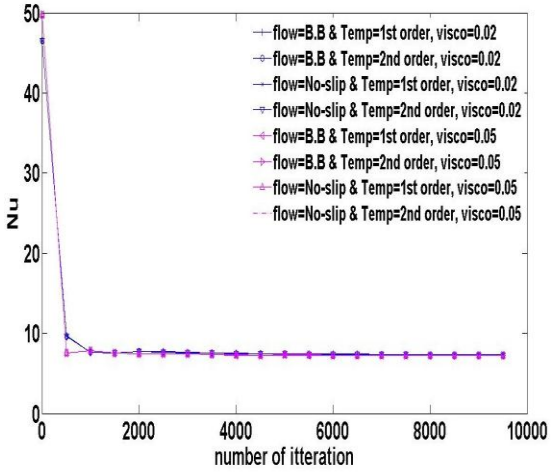

(a)

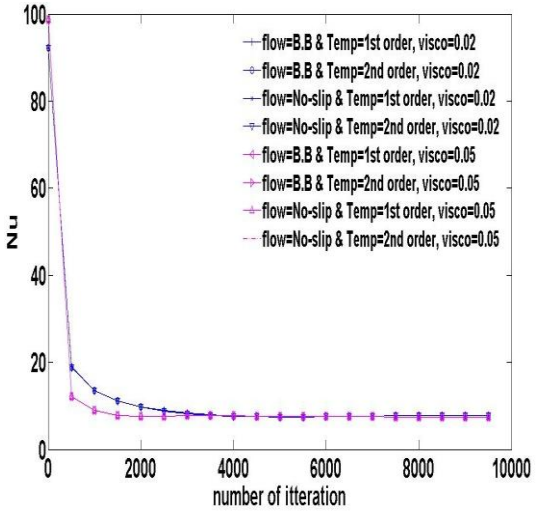

(b)

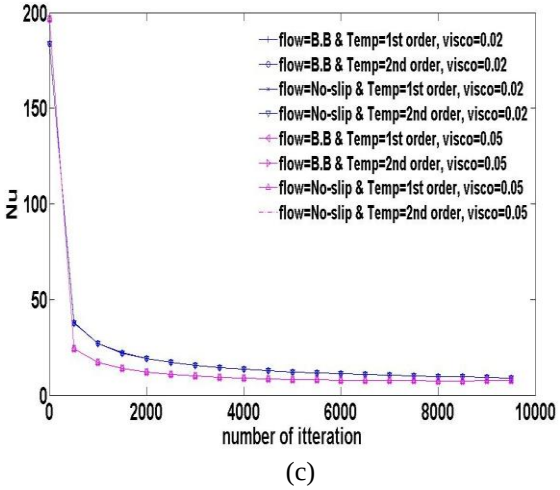

(c)

Fig.13 Nusselt number per iteration using all thermal and hydrodynamic boundary conditions at Ra = 10^5 for the number of lattice nodes on horizontal and vertical walls: a = 64×64, b = 128×128, and c = 256×256.

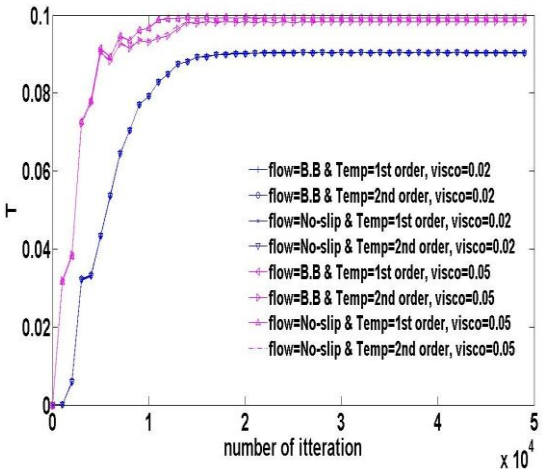

(a)

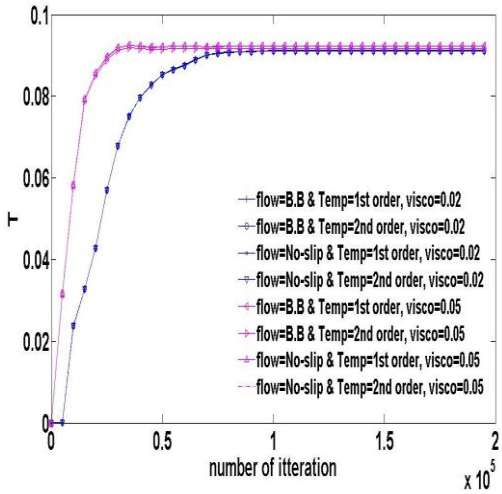

(b)

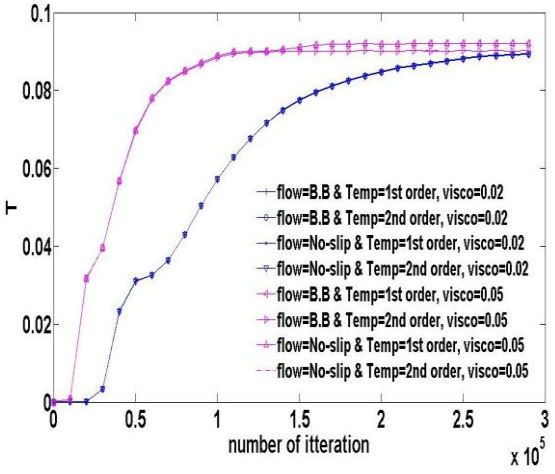

(c)

Fig.14 Temperature at the center of the cavity per iteration using all thermal and hydrodynamic boundary conditions at Ra = 10^5 for the number of lattice nodes on horizontal and vertical walls: a = 128×128 and b = 256×256.

From the results illustrated above, one can see that, in the case of the hydrodynamic boundary condition, both bounce-back and no-slip boundary conditions have similar results. This means that, in a problem with geometry and boundary conditions like this problem, it is convenient to use the simple and less complicated bounce-back boundary condition because, with less cost, the desirable result will be achieved. The same argument can be made for the thermal boundary condition. As it was illustrated in the results, both first- and second-order accuracy thermal boundary conditions have similar outcomes. From these results, one can presume that, in a problem like this one, it is appropriate to use the first-order accuracy boundary condition instead of the more complicated time-consuming second-order one. Finally, it can be claimed that, in such problems as this one (including straight walls), it is convenient to use the first-order accuracy thermal or hydrodynamic boundary conditions and have acceptable outcomes with proper exactness.

5. Conclusion

Comparison results of simulated natural convection in an open-end cavity were studied by applying two different hydrodynamic and two different thermal boundary conditions on solid walls. The results show that the Nusselt number is almost the same in all the different boundary conditions. The temperature at the center of the cavity is also analogous using either of the tested boundary conditions. The temperature also increases as viscosity increases in all cases, and the time steps required to achieve a steady-state solution have a decreasing behavior with increasing viscosity. The decrease in equilibration time with viscosity corresponds to what we would expect, since viscosity is a relaxation parameter. Velocity at the center of the cavity is also almost equivalent in both types of hydrodynamic boundary conditions.

The bounce-back boundary condition is easier to apply because of its simple numerical implementation compared to the no-slip boundary condition. In the no-slip boundary condition, a system of equations needs to be solved on each wall before finding the unknown distribution functions, while in the bounce-back boundary condition, the distribution functions can be found directly. It should be noted that the bounce-back boundary condition is a first-order accuracy method, and it is not desirable to be used with the lattice Boltzmann method, which is a second-order accuracy method. However, as it was observed in the results in Section 4, the difference in the flow velocity and temperature profile between the two methods is not significant, and we can use the bounce-back method instead of the more time-consuming no-slip boundary condition.

The same argument can be made for thermal boundary conditions. As it was observed in the results, both thermal boundary conditions with first- and second-order accuracy have the same effect on the outcomes. Thus, it is appropriate to use the first-order accuracy thermal boundary condition instead of the more complicated and time-consuming one with second-order accuracy. Finally, it can be claimed that, in the geometry with straight walls, it is convenient to use first-order accuracy thermal or hydrodynamic boundary conditions and have acceptable outcomes with proper exactness.

References

[1]. Y. L. Chan, C. L. Tien, A numerical study of two-dimensional natural convection in square open cavities, Int. J. Heat Mass Transfer, vol. 28, No.3, pp. 65–80, 1985.

[2]. E. Bilgen, A. Muftuoglu, Natural convection in an open square cavity with slots, Int. Communications. Heat and Mass Transfer, vol. 35, pp. 896–900, 2008.

[3]. T. Inamuro, M. Yoshino, F. Ogino, A non-slip boundary condition for lattice Boltzmann simulations, Phisics of Fliuds, vol. 7, pp. 2928–2930, 1995.

[4]. R. S. Maier, R. S. Bernard, D. W. Grunau, Boundary conditions for the lattice Boltzmann method, Phys. Fluids, vol. 8, pp. 1788–1801, 1996.

[5]. Q. Zou, X. He, On pressure and velocity boundary conditions for the lattice Boltzmann BGK model, Phys. Fluids, vol. 9, pp. 1591–1598, 1997.

[6]. C. Chang, C. H. Liu, C. A. Lin, Boundary conditions for lattice Boltzmann simulations with complex geometry flows, Computers & Mathematics with Applications, vol. 58, Issue 5, pp. 940–949, 2009.

[7]. I. Ginzburg, Generic boundary conditions for lattice Boltzmann models and their application to advection and anisotropic dispersion equations, Advances in Water Resources, vol. 28, pp. 1196–1216, 2005.

[8]. V. Sofonea, R. F. Sekerka, Boundary conditions for the upwind finite difference Lattice

Boltzmann model: Evidence of slip velocity in micro-channel flow, J. Computational Physics, vol. 207, pp. 639–659, 2005.
[9]. P. A. Skordos, Initial and boundary conditions for the lattice Boltzmann method, Phys, Rev. E, vol. 48, pp. 4823–4842, 1993.
[10]. A. D'Orazio, M. Corcione, G. P. Celata, Application to natural convection enclosed flows of a lattice Boltzmann BGK model coupled with a general purpose thermal boundary condition, Int. J. Thermal Sci, vol. 43, pp. 575–586, 2004.
[11]. M. A. Gallivan, D. R. Noble, J. G. Georgiadis, R. O. Buckius, An evaluation of bounce-back boundary condition for lattice Boltzmann simulations, International journal for numerical methods in fluids, vol.25, pp. 249–263, 1997.
[12]. Z-L. Guo, C-G. Zheng, B-C. Shi , Non-equilibrium extrapolation method for velocity and pressure boundary conditions in the lattice Boltzmann method, Chinese Phys. vol.4, No.11, pp. 366–374, 2002.
[13]. D. P. Zeigler, Boundary condition for lattice Boltzmann simulations, Journal of statistical physics, vol.71, Nos.5/6, pp. 1171–1177, 1993.
[14]. D. R. Noble, S. Chen, J. G. Georgiadis, R. O. Buckius, A consistent hydrodynamics boundary condition for the lattice Boltzmann method, Phys. Fluids, vol. 7, No. 1, pp. 203–209, 1995.
[15]. S. Chen, D. Martnez, R. Mei, On boundary conditions in lattice Boltzmann methods, Phys. Fluids, vol. 8, No. 1, pp. 2527–2536, 1996.
[16]. G. H. Tang, W. Q. Tao, Y. L. He, Thermal boundary condition for the thermal lattice Boltzmann equation, Physical Review, E, Vol. 72, pp. 016703.1–016703.6, 2005.
[171]. H. Huang, T. S. Lee, C. Shu, Thermal curved boundary treatment for the thermal lattice Boltzmann equation, International Journal of Modern Physics C, vol. 17, No.5, pp. 631–643, 2006.
[18]. L. Zheng, Z. L. Guo, B. C. Shi, Discrete effects on thermal boundary conditions for the thermal lattice Boltzmann method in simulating micro scale gas flows, Europhysics Letters, vol. 82 ,No. 4, pp. 44002, 2008.
[19]. M. Corcione, Effects of the thermal boundary conditions at the sidewalls upon natural convection in rectangular enclosures heated from below and cooled from above, International. J. Thermal Sci, vol. 42, No. 2, pp. 199–208, 2003.
[201]. A. D'Orazio, S. Succi, Boundary conditions for thermal lattice Boltzmann simulations, Lecture Notes Comput. Sci, vol. 2657, pp. 977–986, 2003.
[21]. A. D'Orazio, S. Succi, Simulating two-dimensional thermal channel flows by means of a lattice Boltzmann method with new boundary conditions, Future Generation Computer Systems, vol. 20, pp. 935–944, 2004.
[22]. L. S. Kuo, P. H. Chen, Numerical implementation of thermal boundary conditions in the lattice Boltzmann method, Int. J. Heat and Mass Transfer, vol. 52, pp. 529–532, 2009.
[23]. A. A. Mohamad, R. Bennacer, M. El-Ganaoui, Lattice Boltzmann simulation of natural convection in an open ended cavity, Int. J. Thermal Sci, vol.48, pp. 1870–1875, 2009.
[24]. H. N. Dixit, V. Babu, Simulation of high Rayleigh number natural convection in a square cavity using the lattice Boltzmann method, Int. J. Heat and Mass Transfer, vol. 49, pp. 727–739, 2006.
[25]. A. A. Mohamad, R. Bennacer, M. El-Ganaoui, Double dispersion, natural convection in an open end cavity simulation via Lattice Boltzmann Method. Int. J. Thermal Sci, vol. 49, pp. 1944–1953, 2010.
[26]. M. C. Sukop, D. T. Thorne.Jr, Lattice Boltzmann Modeling, Springer-Verlag, Berlin, 2006.
[27]. S. Succi, The Lattice Boltzmann Equation for Fluid Dynamics and Beyond, Clarendon Press, Oxford, London, 2001.
[28]. J. Wang, M. Wang, Z. Li, A lattice Boltzmann algorithm for fluid–solid conjugate heat transfer, Int. J. Thermal Sciences, vol. 46, pp. 228–234, 2007.
[29]. A. A. Mohamad, A. Kuzmin, A critical evaluation of force term in lattice Boltzmann method, natural convection problem. Int. J. Heat and Mass Transfer, vol. 53, pp. 990–996, 2010.
[30]. A. A. Mohamad, Natural convection in open cavities and slots, Numer. Heat Transfer, vol. 27, pp. 705–716, 1995.
[31]. J. F. Hinojosa, R. E. Cabanillas, G. Alvarez, C. E. Estrada, Nusslet number for the natural convection and surface thermal radiation in a square tilted open cavity, Int. Comm. Heat Mass Transfer, vol. 32, pp. 1184–1192, 2005.